Tryptophan-like fluorescence as a fingerprint of urban river water intrusion into storm drainage system

Hailong Yin (yinhailong@tongji.edu.cn)
College of Environmental Science and Engineering, Tongji University https://orcid.org/0000-0002-4112-3731

Yue Wang
Tongji University

Yang Yang
DHI Water and Environment

Jingshui Huang
Helmholtz Center for Environmental Research

Zuxin Xu
Tongji Univeristy

Research

Keywords: storm drainage system, dry-weather misconnection, river water intrusion, fluorescence spectroscopy, Bayesian mass balance model

Posted Date: January 7th, 2020

DOI: https://doi.org/10.21203/rs.2.20179/v1

Version of Record: A version of this preprint was published at Environmental Sciences Europe on April 9th, 2020. See the published version at https://doi.org/10.1186/s12302-020-00336-3.

Tryptophan-like fluorescence as a fingerprint of urban river water intrusion into storm drainage system

Hailong Yin [a,b,c*], Yue Wang [a,b], Yang Yang [d], Jingshui Huang [e*], Zuxin Xu [a,b,c]

[a] Key Laboratory of Yangtze River Water Environment, Ministry of Education, Tongji University, Shanghai, China, 200092

[b] State Key Laboratory of Pollution Control and Resource Reuse, Tongji University, Shanghai, China, 200092

[c] Shanghai Institute of Pollution Control and Ecological Security, Shanghai, China, 200092

[d] Danish Hydraulic Institute, Shanghai Branch, 4th Floor,Building A, No.181 Guyi Road, Shanghai, China, 200235

[e] Department of Aquatic Ecosystem Analysis and Management, Helmholtz Centre for Environmental Research – UFZ, Brückstraße 3a, 39114 Magdeburg, Germany

*Corresponding author. E-mail address: yinhailong@tongji.edu.cn; huangjingshui@126.com

Abstract

Inappropriate dry-weather misconnections into storm drainage system is a demanding environmental problem worldwide. Especially river water intrusion into storm drains may cause the overloading of storm pipes and unexpected serious dry-weather discharge. In this study, we evaluated the possibility of quantifying proportional source contribution in a storm drainage system with dry-weather misconnections from domestic sewage and river water inflow, using rapid and low-cost fluorescence spectroscopy methods. For this purpose, samples of both misconnection sources and outflows of storm drainage system were collected and analyzed in a downtown catchment of Shanghai, China. Results showed that fluorescent peak intensity of tryptophan-like T_1 in domestic sewage (802±126 a.u.) was significantly higher than that in urban river water (57±12 a.u.), while fluorescent peak intensities of tryptophan-like T_2 in urban river water (998±187 a.u.) was much higher than that in domestic sewage (241±72 a.u.) due to increased phytoplankton or algal activity in the polluted water. However, only Peak T_2 passed the conservative behavior test in the incubation experiments, which could be used as a fingerprint for quantitatively identifying the misconnections of urban river water intrusion. We further developed a Bayesian fluorescence mass balance model (FMBM) to infer the percentage of dry-weather misconnections into the storm drainage system as a function of fluorescence intensities of Peak T_2 in the samples of sources and outflows. It was found that the maximum posteriori probability estimate of the percentage of river water intrusion into the storm drains was up

to 20.8% in this site, which was validated by the results of on-site investigation. Our findings implied that in-situ fluorescent sensors and Bayesian FMBM for the fingerprint fluorescence peak could be applied to fast track urban river water intrusion into storm drainage system from both qualitative and quantitative perspective with low costs.

Keywords: storm drainage system, dry-weather misconnection, river water intrusion, fluorescence spectroscopy, Bayesian mass balance model

Background

In order to mitigate overflow pollution of combined sewer systems, separate stormwater system has been introduced since the 1970s, which is designed to delivers clean rain or storm water to the surface water system only [1]. However, the stormwater outfalls can become polluted, for example, when foul water outlets from residential or industrial premises are inappropriately connected to storm water system [2-5]. Such phenomenon leads to the release of untreated sewage into receiving waters, inducing urban water pollution. Additionally, there is also unexpected river water intrusion into storm drains, placing increased burdens on conveyance and the following hydraulic overloading of storm pipe network. This may trigger the storm pumps operation on dry-weather days and result in more serious urban river pollution, e.g., river's black and odorous occurrence [6-7]. Given the mixed surface water and sewage water inputs, there will inevitably be difficulties in specifically distinguishing between misconnection-derived sewage and surface water sources, when monitoring and analyzing a storm drain outfall.

Use of chemical tracers is a promising method to detect misconnected source flow

63 contributions into storm drains. Specifically more and more researchers have shed light on
64 chemical or biological marker species to identify and quantify sewage source discharge.
65 For example, many researchers demonstrated that PPCPs, artificial sweeteners and
66 inorganic ions such as potassium, chloride and sodium, could serve as promising markers
67 of sewage contamination [8-16]. However, no published literatures were found concerning
68 the use of markers in identifying surface water intrusion into the storm pipes. Additionally,
69 current use of above chemical or biological markers is still less easily automated for higher
70 throughputs especially in a catchment-scale condition assessment.

71 Compared with the chemically and biologically based analytical methods, fluorescence
72 spectroscopy has the advantages of high sensitivity, simple measurement, fast analysis, low
73 sample size request and no secondary pollution, which provides both qualitative and
74 quantitative information of dissolved organic matter (DOM) in natural and engineered
75 systems [17-20]. Three-dimensional excitation-emission (EEM) fluorescence, has been
76 widely used to quantitatively characterize DOM and to follow its dynamics in different
77 aquatic environments, e.g., in rivers [21-25], estuaries or seawaters [26-28], lakes [29-32],
78 wastewater effluents [33] and groundwater [34]. Such studies concluded that fluorescence
79 characteristics of DOM varied in different water bodies. Thus, by examining them, it is
80 possible to distinguish different sources of DOM and determine the presence of different
81 sources in water bodies of concern.

82 In urbanized areas, while an increasing number of studies had characterized and traced
83 the sources of DOM using fluorescence spectroscopy to explore the influences of urban
84 landscapes and environmental factors on the urban waterbodies, few related studies
85 focused on the DOM fluorescence characterization of sewer overflows, a fact that may be

ascribed to the complexity of wet-weather and dry-weather pollutants. Chen et al. [35] investigated the changes of the wet-weather flow DOM characteristics and yields in response to the anthropogenic influences of paved runoff and sanitary sewage inputs. However, no published literatures were found regarding the dry-weather misconnections into storm drainage system, a phenomenon arising from the complexity of mixed non-storm water flow inputs.

The aim of this study was to qualitatively and quantitatively identify contributions from different sources of dry-weather misconnections into storm drainage system using fluorescence detection. The derived outcomes are expected to inform a methodology that can be directly applied to fast diagnose the in situ dry-weather misconnections, especially for the quantification of surface water intrusion into the storm drains.

Materials and methods

Site description

The study site is a typical high-density urbanized area (approximate 270 capital/ha) in Shanghai's downtown area, surrounded by three tidal rivers (i.e., the Puhuitang, Shang'aotang and Caohejing river) (Fig. 1). Covering 374 ha, this area is served by separate sewer and storm drainage system that was built in 1980s. There is only one terminal outfall for the storm drainage system, where a storm pump station has been constructed to convey the surface road runoff in wet-weather days to the receiving waters. However, non-storm water flows including domestic sewage as well as surface water also find their ways into storm drains.

On-site investigation showed that there were potential 99 misconnections between river

and storm drains in this catchment [6]. On dry-weather days, when surface water level is higher than the water level of terminal outfall (i.e., during high tide of the surrounding tidal rivers), river water intrusion into storm drains occurs and may even trigger storm pumps operation, delivering untreated sewage into the nearby rivers.

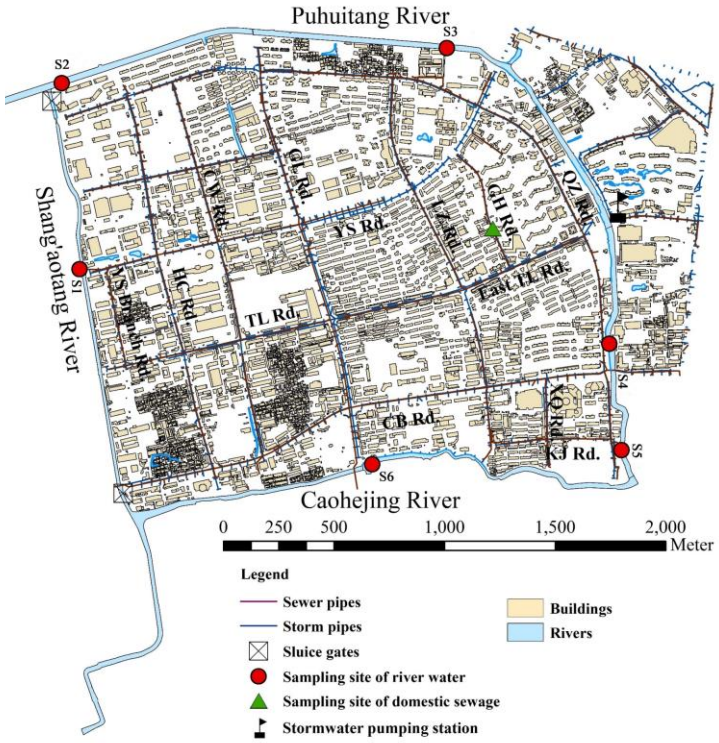

Fig. 1 Study site description

On-site sampling methods

Sampling activities were conducted during 16th November, 2011 to 31st January, 2013. For the potential misconnected entries as well as the dry-weather catchment outflow, sampling methods were described as below.

Sampling of domestic sewage. Sewage samples were collected from the sewer outlet of one residential community, which was inappropriately connected to the storm drain (see Fig.1). An automatic sampler (ISCO 6712C, Teledyne, Lincoln, Nebraska, USA) was used

to collect the water sample by choosing the “1-h equal interval sampling” program, and 24 h was set as a sampling cycle. The mixture of the 24 water samples was used for each sampling activity. All together 18 sampling activities were conducted and correspondingly 18 composite sewage samples were obtained.

Sampling of river water. The river water sampling sites were located in the three tidal rivers surrounding this catchment, i.e., Puhuitang, Shang'aotang, and Caohejing rivers, where six sampling sites were selected (see Fig.1). At each sampling site, water samples were collected 0.5 m below the water surface in the midstream of the watercourse. For each sampling event, one river water sample was collected at each monitoring station. Totally 15 sampling activities were performed and 90 river water samples were obtained.

Sampling of catchment outflow. For the catchment outflow, the antecedent dry weather period of 48 h was chosen before the start of each sampling campaign. Therefore, the contribution of potential storm water runoff to the catchment outflow could be excluded. Water samples were extracted from the terminal wet well using an ISCO 6712 automatic field sampler. Like the sewage samples, outflow samples were collected every hour by choosing the “1-h equal interval sampling” program, and 24 samples were obtained within each day. Finally, the mixture of 24 water samples was used for the experiment analysis for each sampling activity. Totally 12 sampling activities were performed.

All of the collected water samples were stored in the pre-washed and dried sampling bottles. After being transported to the laboratory, the samples were immediately filtered through a 0.45-μm microporous membrane. The filtered samples were stored at 4°C in the dark before analysis. The measurements were completed within 48 hours.

146 **Analytical methods**

147 Fluorescence detection was carried out using Hitachi three-dimensional fluorescence
148 spectrophotometer F-4600. Each sample was placed into a 1-cm quartz cuvette for
149 detection and blank corrected. The scanning parameters were set as follows: the
150 photomultiplier tube (PMT) voltage was 700 V, and the scanning speed was 12000
151 nm•min^{-1}. The ranges of excitation wavelength (Ex) and emission wavelength (Em) was
152 200-450 nm and 250-550 nm respectively, with the step size of 5 nm.

153 Several post-acquisition steps were used to adjust the EEM data. First, the excitation and
154 emission data were corrected for instrument-specific response. Second, the EEM response
155 of ultrapure water was subtracted from sample EEMs. Third, the UV−visible absorption
156 spectra were used to correct the EEM data for inner filter effects.

157 Peak-picking is a viable analysis technique used for the development and use of a real-
158 time tool, which can be directly tied to custom sensors available today [19,22,33,36].
159 Commonly there are four kinds of fluorescence peaks observed in freshwater aquatic
160 samples. These have been classified as follows: Peak A – fulvic-like ($\lambda_{ex/em}$=237-260/400-
161 500 nm); Peak C – humic-like ($\lambda_{ex/em}$=300-370/400-500 nm); Peak T_1 – tryptophan-like
162 ($\lambda_{ex/em}$=275/340-350 nm) and Peak T_2 – tryptophan-like ($\lambda_{ex/em}$=225-237/340-381 nm);
163 Peak B_1 – tyrosine-like ($\lambda_{ex/em}$=275/300-305 nm) and Peak B_2 – tyrosine-like ($\lambda_{ex/em}$=225-
164 237/309-321 nm). The Peak C fluorescence can be further divided into two fluorescence
165 centres in highly coloured, peaty waters. Specifically, fluorescence is reported to occur at
166 $\lambda_{ex/em}$=320-340/410-430 nm and at $\lambda_{ex/em}$ =370-390/460-480 nm, which are referred to as
167 Peak C_1 and C_2 respectively.

168

Lab incubation experiment setup

Besides on-site sampling to detect fluorescence components of the study site, in order to determine the conservative behavior or not of the detected DOM fluorescence, lab experiments were also conducted.

Usually storm drains are designed to accommodate urban surface runoff, which means they are often oversized for dry-weather flow inappropriately entering the storm pipes. Therefore, the dry-weather flowing velocity within the storm drains would be very low. In this catchment, it was estimated that dry-weather water flowing velocity was below 0.1 m/s; correspondingly, the maximum travel time of dry-weather flow (e.g., sewage or river water) within the storm network was about 24 hrs [37]. In order to simulate the actual environment in the sewer, a continuous darkroom anaerobic condition for more than 24 hours was used in the laboratory incubation experiment. Specifically, sewage or river water samples were respectively injected into a series of 250mL borosilicate glass bottles, which were sealed with parafilm and wrapped with foil to represent anoxic and dark environment. For each experiment, the duration was equal or greater than 24 hrs. The fluorescence was measured before the experiment and at 24-h interval during the incubation experiment.

The experiments were performed both in the spring and winter seasons to determine the effect of environmental temperature and associated microbial activities on the conservative behavior of detected DOM components. In details, the incubation experiments were conducted for the collected sewage samples in May, 2012 (i.e., the period of spring season) and January, 2013 (i.e., the period of winter season). The experiment temperatures were controlled close to the environment temperatures in the two seasons, namely with 25^0C for the incubation experiment in May and 5^0C for the one in January.

Fluorescence Mass Balance Model

Hudson et al. pointed out that fluorescence intensities of the peaks in the specific regions of the EEM could correspond to the concentrations of the compounds represented by the peaks [38]. Goldman et al. further found a linear response in fluorescence peak intensity of individual peaks (e.g., Peaks A, T and C) for the mixture of different source flows [22]. In accordance with these criteria, for a fluorescent component exhibiting conservative behavior, i.e., no obvious chemical or biological degradation within the storm drains, the fluorescence mass balance equation can be written as:

$$F_{river} \times Q_{river} + F_{sewage} \times Q_{sewage} = F_{outflow} \times Q_{outflow} \quad (1)$$

where F_{river} is the fluorescence intensity of the peak for river water samples; Q_{river} is the flow rate of river water intrusion into the storm drains; F_{sewage} is the fluorescence intensity of the peak for domestic sewage samples, Q_{sewage} is the flow rate of domestic sewage misconnected into the storm drains; F_{outflow} is the fluorescence intensity of the peak for catchment outflows; Q_{outflow} is the flow rate of the storm drain outfall on dry-weather days.

Assuming that the percentage share of river water intrusion into the storm drains on dry-weather days is r (%), the following formula could be derived from the above mass balance model as:

$$\begin{aligned} F_{river} \times Q_{outflow} \times \mathrm{r} + F_{sewage} \times Q_{outflow} \times (1 - r) \\ = F_{outflow} \times Q_{outflow} \end{aligned} \quad (2)$$

Divided by Q_{outflow}, the model of fluorescence intensities and the percentage share of river water intrusion into the storm drains can be generated as:

$$F_{sewage} + r \times (F_{river} - F_{sewage}) = F_{outflow} \quad (3)$$

A Bayesian method was employed here to infer *r*, which is capable of accounting for the measurement errors of fluorescence intensities and estimate the uncertainty of the percentage share [39]. A widely used Markov Chain Monte Carlo (MCMC) approach was integrated with the model using DREAM [40]. Normal distribution tests were performed with the measurements of F_{river}, F_{sewage} and $F_{outflow}$ to obtain the means and standard deviations of their distributions, respectively. F_{river}, F_{sewage} and *r* were defined as the input parameters in the model. The prior information of F_{river} and F_{sewage} was provided by the estimates of their normal distribution parameters, respectively. A uniform probability density function (PDF) between 0 and 1 was considered for the prior distribution of *r*. $F_{outflow}$ is defined as the output of the model. The model parameter inferences were based on the log-likelihood function:

$$logL = -\frac{M}{2}log(2\pi) - \sum_{i=1}^{M} log\sigma_i - \frac{1}{2}\sum_{i=1}^{M}\frac{1}{{\sigma_i}^2}(F_i^{obs} - F_i^{sim})^2 \quad (4)$$

where *i* and *M* donate the i^{th} measurement and the number of measurements, respectively; F^{obs} and F^{sim} are observed and simulated $F_{outflow}$, respectively; σ denotes the standard deviation of the Gaussian distribution of observed $F_{outflow}$.

Results and Discussion

The EEMs from samples collected from the domestic raw sewage and urban river water have been evaluated and show 3 peaks (T_1, T_2, B_1) with the strongest fluorescence intensities (Fig.2). More information concerning the EEM spectra of these samples

collected was listed in Supporting Information S1 and S2 for domestic sewage and river water respectively.

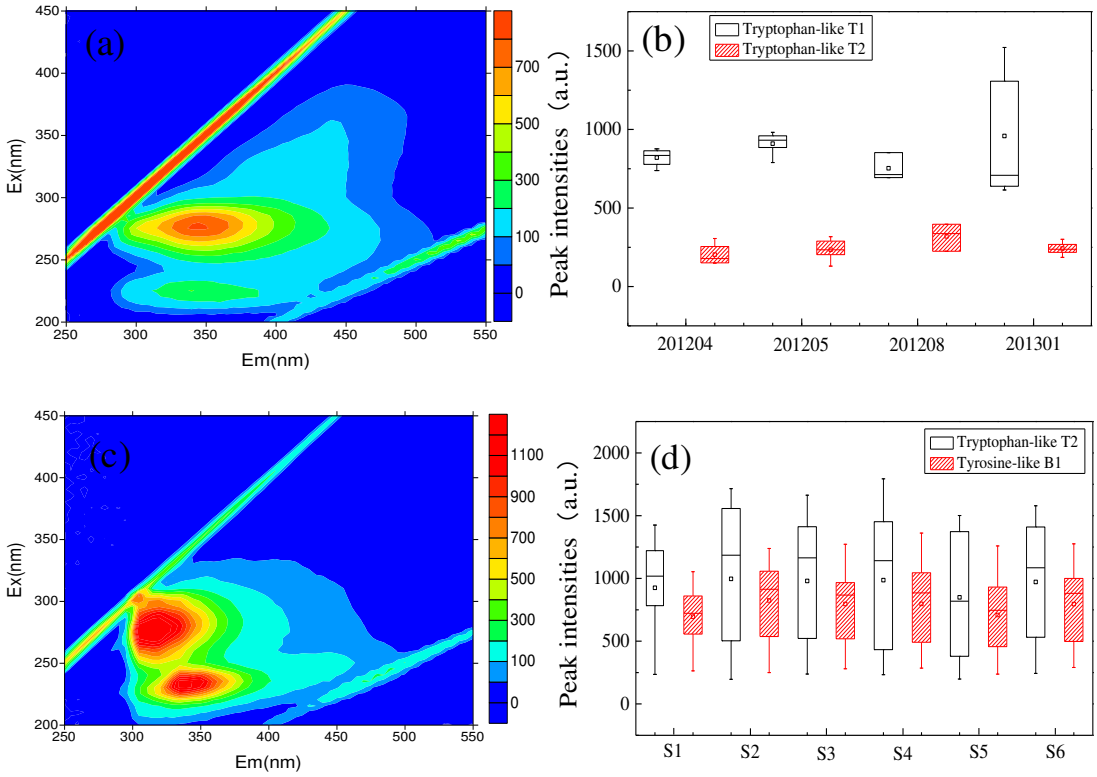

Fig.2 Detected EEMs for the domestic sewage and urban river water samples: (a) typical EEM of untreated domestic sewage; (b) fluorescent peak intensities of domestic sewage samples; (c) typical EEM of urban river water; (d) fluorescent peak intensities of urban river water at six sampling stations.

EEM characteristics of domestic sewage

Fig.2(a) showed that basically there were two main fluorophores in the spectrum of domestic sewage. The first fluorescence intensity peak was at Ex/Em of 275/350 nm, which corresponded to tryptophan-like peak T_1 components. The second fluorescence intensity peak was at Ex/Em of 225/350 nm, which was associated with tryptophan T_2 fluorescent

243 components. The detected tryptophan-like fluorescent components are mainly protein-like
244 substances, which may be derived from the human activities such as human excreta, food
245 residues and cooking oils [41]. In addition, a distinct narrow band occurred at λ_{ex}=330-
246 375 nm for λ_{em}=410-450 nm. This is can be explained by the fluorescent whitening agents
247 from the grey water such as dishes and clothes washing, which also indicates the
248 contribution of the domestic sewage to some extent. Considering domestic sewage is
249 transported through pipelines and has no direct contact with soil, the possibility of humus
250 from the soils is small. Therefore, the humic-like fluorescent components in domestic
251 sewage are mainly derived from the humic acids originated in tap water supply. From this
252 perspective, the intensity of humic-like substances were much less pronounced than the
253 protein-like ones in the domestic raw sewage samples.
254 Based on Fig.2(b), the averaged fluorescent peak intensity of tryptophan-like T_1 and
255 tryptophan-like T_2 material were 865 a.u. and 256 a.u respectively, with an average T_1/T_2
256 ratio of 3.4. Hudson et al. [17] observed an approximate T_1/T_2 ratio of 3.0 for samples
257 collected from sewage effluents, close to the data from our study. In Fig.2(b), increased
258 fluorescent peak data for T_1 was associated with organic matter of oils. For example, real-
259 time fluorescent peak data in a small urban river recorded by Carstea et al. [19], showed
260 that the fluorescent ratio between T_1 and T_2 rose to 4~5 from previous 1.7~3.5 during the
261 diesel pollution. Chen et al. [41] presented the T_1/T_2 ratio of soybean oil was 3.8, whereas
262 in bovine serum albumin (i.e., a standard substance in protein quantitation) the data was
263 only 1.0. Therefore, peak T_1 is identified as being most likely to be the signature of
264 domestic sewage.
265

EEM characteristics of river water

As indicated in Fig.2(c), there were two distinct fluorescence peaks in the EEMs of the river water samples, with the Ex/Em at 230/340 nm and 275/305 nm respectively. The peak at EEM of 230/340 nm corresponds to tryptophan-like T_2 materials, and the peak at EEM of 275/305 nm corresponds to tyrosine-like B_1 materials. Both the tryptophan-like T_2 and tyrosine-like B_1 belong to protein-like materials.

As for the humic or fulvic substance, a fluorophore was also generated at with the Ex/Em at 250/435-455 nm. However, its fluorescence intensity was not as high as that of tryptophan-like T_2 and tyrosine-like B_1 substances in this case. Previous studies by Hudson et al. [38] showed that in clean rivers, Peaks C_1, C_2 and A predominate. This is because DOM originating from clean river water is dominated by natural organic matter from plant material whereas sewage-derived DOM is dominated by organic matter originating from microbial activity. By contrast, our study showed that tryptophan-like or tyrosine-like substances, instead of humic-like or fulvic-like substances, are the indication of polluted urban river water. Therefore, with increasing urbanization and anthropogenic activities, the fluorescent signature of urban waters changed with increasing human impact from humic-rich to protein-rich with Peaks T and B.

Fig.2(d) further showed the measured fluorescent peak intensities of urban river water at six sampling stations. Among the six sites, the S1 monitoring site is located in Shang'aotang River, where sluice gates are installed (see Fig.1). As a result, Shang'aotang River is separated from other rivers including Puhuitang River and Caohejing River, which are polluted by the dry-weather as well as wet-weather outflow from the storm drains of this catchment. By contrast, no storm drains outfalls are directly connected to the

289 Shang'aotang River. Therefore, water quality at S1 station was better than that of the other
290 five sampling stations. However, the fluorescence intensities of tryptophan-like T_2 and
291 tyrosine-like B_1 at the S1 station were not considerably different from those at other five
292 stations. This showed that fluorescence property of urban polluted rivers was determined
293 by materials more than sewage-derived DOMs.

294 **Differences of EEM characteristics between domestic sewage and urban river water**

295 Our study showed that domestic sewage featured most strongly tryptophan-like Peaks T_1
296 and T_2, whereas urban river water featured tryptophan-like Peak T_2 and tyrosine-like Peak
297 B_1. Both domestic sewage and urban river water are characteristics of tryptophan-like T_2
298 fluorescence; however, it was interesting that tryptophan-like Peak T_2 in the urban river
299 water was more intense than that in the untreated domestic sewage.

300 Fig.3 showed that organic matter in the investigated urban rivers exhibited seasonally
301 different fluorescence intensities over the sampling period. Tryptophan-like Peak T_2 as well
302 as tyrosine-like Peak B_1 was observed to be more intense in winter as compared to that in
303 summer. This was related to elevated river water levels due to stormwater runoff discharge
304 into rivers and resulting dilution effect in summer to some extent. However, even diluted
305 by stormwater runoff, fluorescence intensities in Peaks T and B of river water samples were
306 still higher than those of sewage samples. The explanation is Peaks T and B are related to
307 microbial activity [42] and may be transported into a system (allochthonous) or be created
308 by microbial and biological activity within a system (autochthonous). Intensive
309 tryptophan-like T_2 and tyrosine-like B_1 are related to biological activity particularly in
310 areas of high primary productivity, that is, surface waters with phytoplankton or algal
311 activity. Under this circumstance, tryptophan-like T_2 and tyrosine-like B_1 fluorescence may

312 be present as ‘free’ molecules or else bound in proteins or humic structurers of algae cells
313 and their remnants in river waters. In Shanghai area, majority of aquatic plants grow in the
314 spring and summer season and decay in the winter season [43]. Decomposition of aquatic
315 plants contributed to the intensified tryptophan-like T_2 and tyrosine-like B_1 substances.
316 Such explanation could be strengthened by recently reported protein-like fluorescence in
317 Taihu Lake, China, where the tryptophan-like components of DOM were significantly
318 higher in winter than in summer and autumn, due to the degradation of phytoplankton [32].

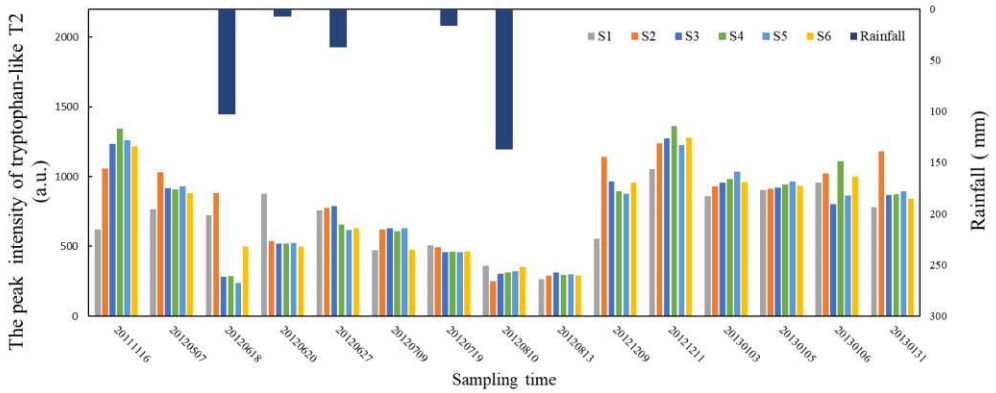

319

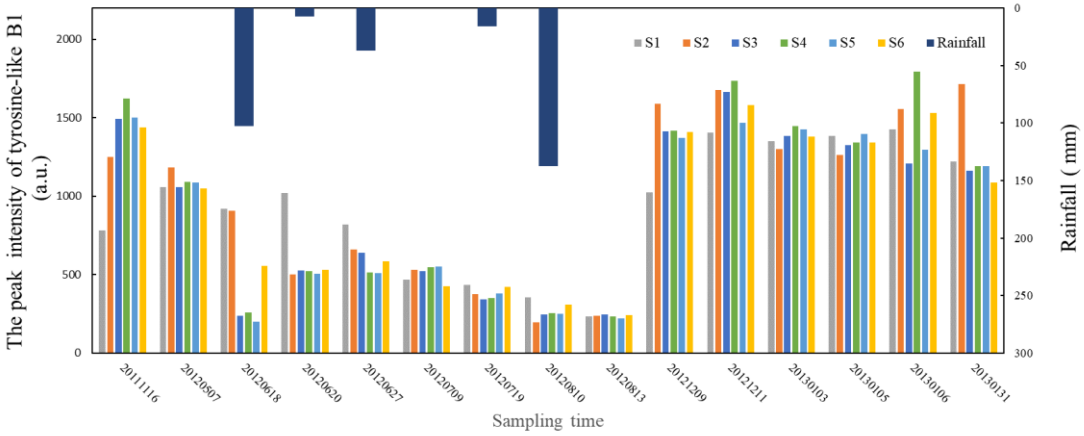

320
321 Fig.3 Detected fluorescence intensities at six sampling sites of the urban river water.

322

323 Another explanation is as follows. Usually, at lower water temperature, dinoflagellate or
324 diatom are predominant algal species; by contrast, at higher water temperature, green algae

and blue algae take the lead in algal growth. Among the algal species, dinoflagellate and diatom are dominant producers of terrestrial sources, featuring higher contents of tryptophan-like and tyrosine-like materials than those in green and blue algae. Moreover, there is a good correlation between Peaks T and B materials produced by algal species of dinoflagellate and diatom [44], as proved by in this study. In this case, a strong liner relationship between the fluorescence peak intensities of tryptophan-like T_1 and tyrosine-like B_1 was demonstrated, with average correlation coefficient of 0.96 ($p<0.01$).

Based on above discussions, higher T_2 fluorescence intensity observed in the urban river water was due to phytoplankton or algal related activity in the polluted urban river. Specifically, if excluding the river fluorescent data disturbed by stormwater runoff in sampling period of summer season, average T_2 peak intensity in urban river water samples was 998 a.u., but average T_2 peak intensity in untreated domestic sewage was only 241 a.u.. The intensities in Peak T_2 between urban river water and domestic sewage differed by 4.1 times. This revealed that tryptophan-like Peak T_2 would be of great potential for the use in indicating the urban river water and associated river water intrusion into urban drainage system.

Conservative behaviour of fluorescence peaks in sewage and surface water

Changes in observed fluorescence peak intensities of domestic sewage and river water samples during the experiments were shown in Fig.4 and Supporting Information S3. As seen in Fig.4(a) and Fig.4(b), for the domestic sewage samples, lab incubation experiments conducted in May showed fluorescence peak intensities of tryptophan-like T_1 and tyrosine-like B_1 decreased over time rapidly with the experimental duration. Fluorescence intensity of Peak T_1 and B_1 decreased by 70.8% and 66.1% respectively on average after 24 hrs. In

348 this process, fluorescence intensities of other fluorescent components did not increase
349 correspondingly (see Supporting Information S3). This result indicated that the
350 fluorescence intensities of the tryptophan-like T_1 and tyrosine-like B_1 substances converted
351 into non-fluorescent substances with time. As discussed above, the tryptophan-like T_1 and
352 tyrosine-like B_1 component in domestic sewage were considered to be microbial by-
353 products, and therefore changes in their fluorescence intensities were related to microbial
354 metabolism. For this scenario under the lab temperature of 25^0C, active microbial activity
355 dramatically degraded their fluorescent substances. Reynolds concluded that microbial
356 activity, measured by oxygen depletion in the BOD_5 test, correlates well with the T_1
357 fluorescence intensity of raw sewage [45]. Therefore T_1 is presented in a bioavailable
358 substrate. However, for the incubation experiments conducted in January, the fluorescence
359 signature of tryptophan-like T_1 and tyrosine-like B_1 component in domestic sewage almost
360 remained unchanged with time. This can be explained by inhibited microbial activity under
361 lower lab temperature (e.g., the temperature of 5^0C), leading to relatively stable
362 fluorescence peak intensities.

363 Changes of fluorescence signature of tryptophan-like T_2 with experimental duration was
364 shown in Fig.4(c) and Fig.4(d) for domestic sewage and surface water samples. For the
365 domestic sewage samples, unlike tryptophan-like T_1 and tyrosine-like B_1 substance,
366 tryptophan-like T_2 exhibited conservative behavior, independent of environmental
367 temperature. The explanation may be that tryptophan-like T_2 substance contains more
368 simple aromatic structurers, which are less likely to be degraded. Our experimental results
369 further strengthened that tryptophan-like T_2 component could be associated with
370 biodegradation of wastewater, i.e., they could be the bio-refractory organics or microbial

byproducts [23]. Similar results were found in experiments of river water samples, in which fluorescence intensities in tryptophan-like T_2 substance also didn't change within the experimental duration of 72 hours. However, while tryptophan-like T_2 component in raw sewage could be cited as anthropogenically derived organics, T_2 component in surface water is believed to be belonging to plankton-derived organics. Especially, there could be higher levels of non-biodegradable organics in urban river than those in untreated domestic sewage.

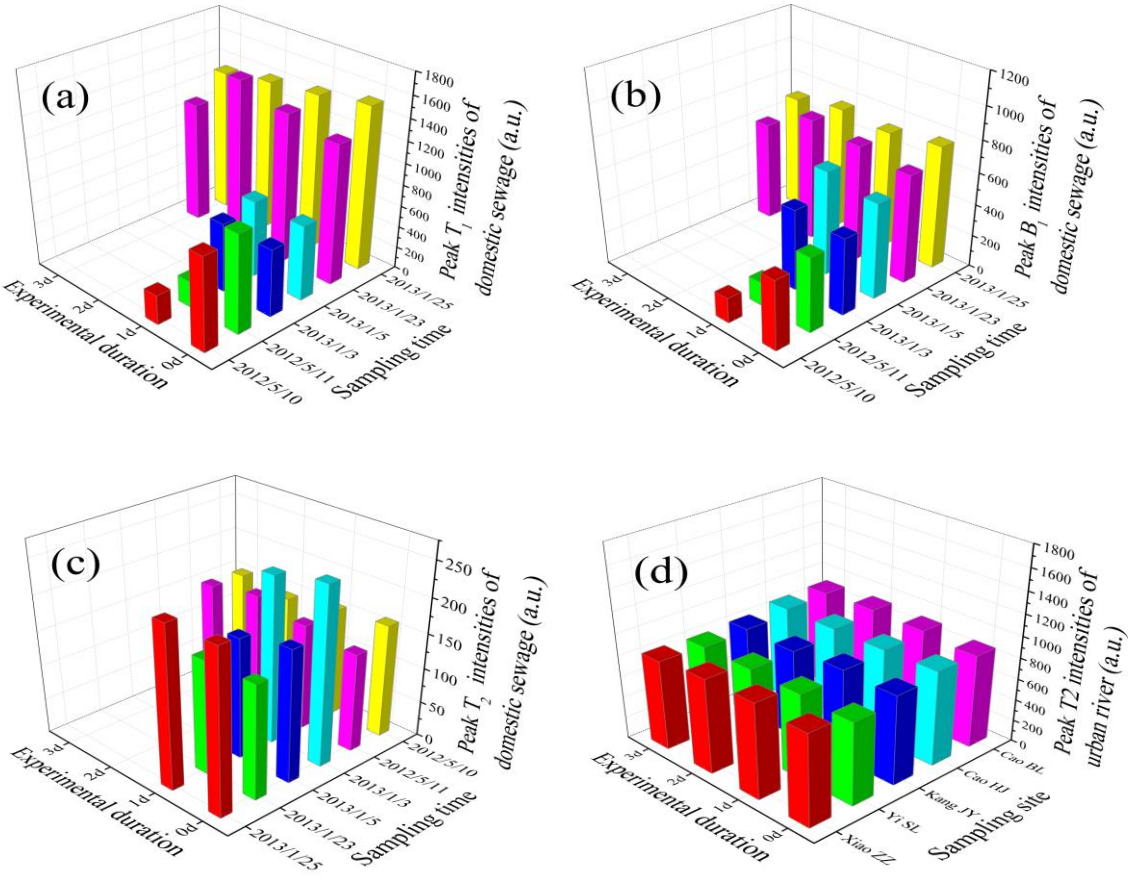

Fig.4 Changes of fluorescence peak intensities of domestic sewage and urban river water samples within the experimental duration.

Based on above discussion, tryptophan-like T_2 can be used as an ideal marker to quantify percent wastewater and urban river water with inappropriate entry into storm drains on dry-weather days, which features conservative characteristics in both of the two misconnected source types. Thus, the uncertainty of fluorescence mass balance model arising from chemical or biological reaction within the storm pipes could be minimized as possible as can.

Determination of percent surface water and wastewater into the storm drains

To determine the percent surface water into storm drains, the fluorescence mass balance model was set up for fluorescence Peak T_2 with its fluorescence intensity measurements of the samples from the river water, domestic sewage and catchment outlet. Comparison of fluorescence Peak T_2 among domestic sewage, river water and catchment outflow was presented in Fig.5. More information concerning detected EEMs for all of the catchment outflow samples were provided in Supporting Information S4.

As seen in Fig.5, for both summer and winter season periods, the fluorescence Peak T_2 intensities in the catchment outflows were higher than those in the domestic sewage, due to occurrence of river water intrusion. For catchment outflow, generally fluorescence intensities of tryptophan-like T_2 in winter were higher than that in summer, as a result of intensified fluorescence Peak T_2 of river water in the winter season period. Therefore, fluorescence spectrometry has the promise for indicating the presence of river water intrusion into storm drains as a rapid, reagentless technique that requires little sample preparation.

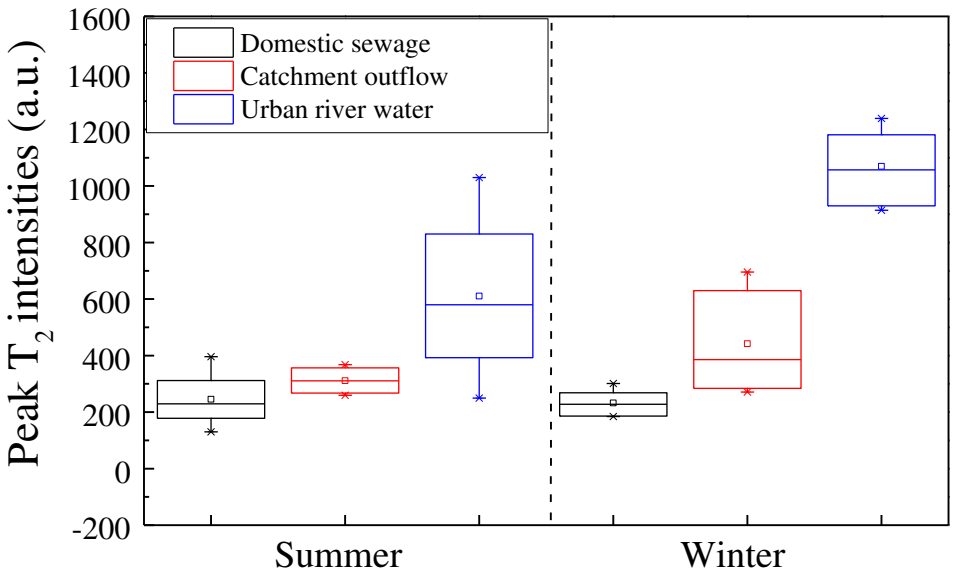

405

406 Fig.5. Comparison of fluorescence peak T_2 intensities for the samples among river water,
407 domestic sewage and catchment outflow.

408

409 The Bayesian inference results of the percent river water into the storm drains for the
410 two season periods were shown in Fig.6. It showed that the maximum a posteriori
411 probability (MAP) estimate of the percent is 12.7% and 20.8% in summer season and
412 winter season respectively. Theoretically, the amount of river water backflow is determined
413 by the pressure head between surface water and storm drains; the higher the river water
414 level, the larger the amount of river water backflow. Therefore, higher MAP in winter was
415 associated with lower water level of storm drains of non-flood season period. However,
416 uncertainty of Bayesian result in summer was higher than that in winter. This is possibly
417 due to frequent rainfall events and intense precipitation during summer season. Storm water
418 discharges led to significant variations of fluorescent substances in the three surrounding
419 rivers (see Fig.5), and the resulting increased uncertainty of percent river water intrusion.

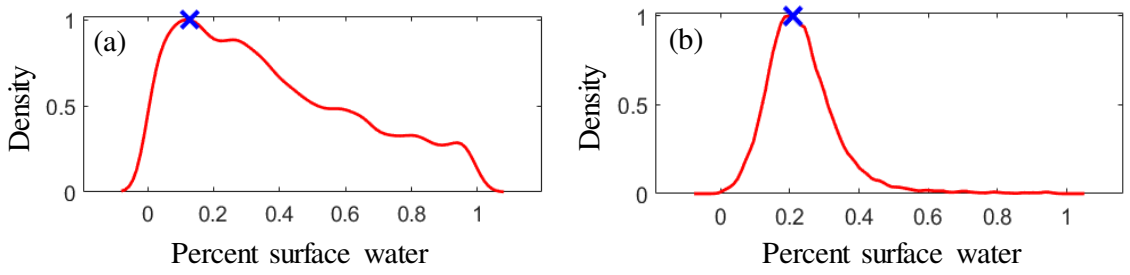

420

421 Fig.6 Maximum a posteriori probability (MAP) estimate for the percentage share of river
422 water backflow into the storm drains on dry-weather days: (a) summer season; (b) winter
423 season.

424

425 The Bayesian inference results were validated with the estimated time-series river water
426 inflow in winter season in this case. Fig.7 showed the measured historical real-time water
427 levels between surrounding rivers and terminal outfall within one month of winter season
428 period (i.e., Dec., 2008). Using the mathematical function between river water inflow and
429 pressure head established in this catchment (i.e., $Q_{river}=0.104*\Delta h^{1/2}$, Q_{river} is river water
430 inflow and Δh is the sum of real-time water pressure head between river water level and
431 terminal wet well level within one day) [6], the daily river water inflow was accordingly
432 determined, as seen in Fig.7. It was known from this figure that when storm pumps operated
433 to lower the terminal wet-well level to the lowest alarm level, the significantly increased
434 pressure head drives large amounts of river water inflow in a short period of time. For the
435 non-pumping discharge periods, river water inflow is much smaller as compared to that
436 under the pumping discharge periods. In this figure, the daily river water inflow ranged
437 from 145~11705 m^3/d, with an average data of 4261 m^3/d.

438 Our previous study showed that catchment outflow on dry-weather days was
439 approximately 19,350~21,600 m^3/d [6]; therefore maximum likelihood value of river water

inflow in winter season was about 4025~4493 m^3/d based on MAP estimate for percent surface water intrusion. The daily averaged river water inflow based on Fig.7 coincided well with the MAP estimate, with a relative error less than 10%. This demonstrates that FMBM is robust in quantifying surface water intrusion into storm drains.

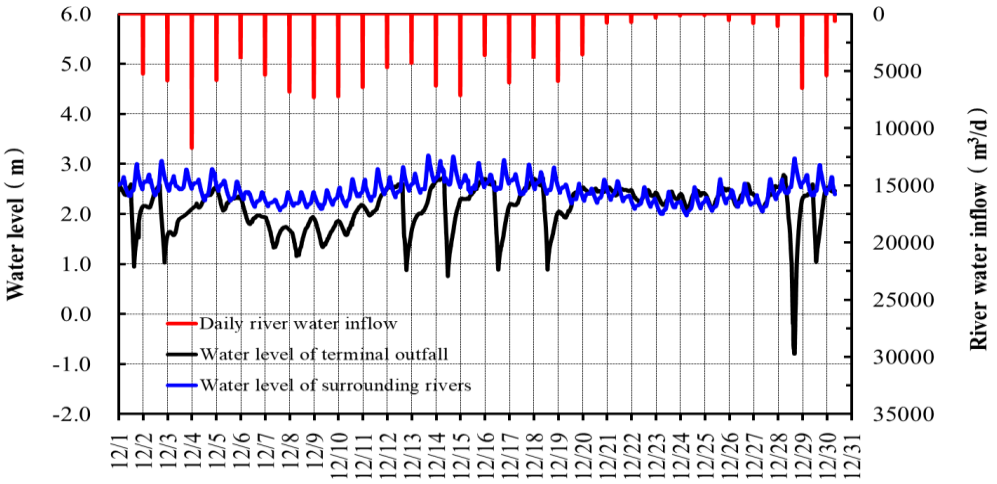

Fig.7 Estimated daily river water inflow into storm drains based on real-time water level between river and catchment outfall in winter season period.

Environmental implications

The use of fluorescence to predict the presence and quantity of urban river water into a storm drainage system has significant environment implications. Recent advancements in sensor technology and the development of reliable and specific fluorescence probes have increased our ability to monitor organic matter characteristics in near real-time. The application of real-time data and fluorescence mass balance model would allow water managers to track and quantify river water inflow without high costs associated with labor-intensive investigations or complex analytical approaches. For example, establishing a fitted analytical function to determine the river water inflow, has to depend on long-term

real-time synchronous flow discharge and pressure head data (river water level versus catchment water level) for each catchment. By contrast, if aided with tryptophan-like T_2 sensor and FMBM introduced in this study, administrative managers would be provided with a useful, fast and cheap alternative way for the investigation of dry-weather misconnections into urban storm drainage system.

The study was conducted on polluted urban rivers, whereas there may be dissimilarities in the organic matter of other surface water bodies or misconnected source types. However, we can develop same approaches to identify and quantify illicit discharges, considering custom sensors have already been constructed to capture the key peaks such as the strong microbial fluorescence signal. Additionally, the presented fluorescence approach could be combined with other chemical tracers to present an in-depth insight into illicit discharge investigation of various source types from a wider perspective, and also determine the best times to perform other chemical analyses if necessary.

Conclusion

In the present study, fluorescence spectroscopy method was used to detect and quantify urban river water from the dry-weather flows that inappropriately entered into the storm drains. Our findings were listed as follows.

The fluorescence spectra of two misconnected sources including domestic sewage and urban river water exhibited substantially different characteristics, with the strongest fluorescence peak centers at an excitation/emission wavelength (Ex/Em) of 275/350 nm (tryptophan-like T_1 fluorescent substances) for the domestic sewage and 230/340 nm (tryptophan-like T_2 fluorescent substances) for the urban river water, respectively.

Results showed that fluorescence peak intensities of tryptophan-like T_1 in domestic

480 sewage (802±126 a.u.) was significantly higher than that in urban river water (57±12 a.u.),
481 while fluorescence peak intensities of tryptophan-like T_2 in urban river water (998±187
482 a.u.) was much higher than that in domestic sewage (241±72 a.u.). Higher T_2 fluorescence
483 intensity observed in the urban river water was associated with the increased phytoplankton
484 or algal activity in the polluted urban river.

485 Lab incubation experiments showed that only Peak T_2 passed the conservative behavior,
486 which could be used as a fingerprint for quantitatively identifying the misconnections of
487 urban river water intrusion. Using the developed Bayesian fluorescence mass balance
488 model (FMBM), the MAP estimate of the percent river water into the storm drains in a
489 downtown catchment of Shanghai, China (3.74 km^2) can be responsible for up to 20.2%.
490 This result has a relative bias less than 10% compared with the averaging values within
491 one month of winter season, derived from real-time water pressure head between river and
492 storm drainage system.

493 Our findings highlighted that the presented Bayesian FMBM approach could be
494 employed to infer the contribution of surface water intrusion into the storm drains. In the
495 future, custom sensors can be installed to real-time analyze the fingerprint fluorescence
496 peak in the storm drainage system. The application of real-time fluorescence data and
497 Bayesian FMBM method should allow urban water manager to track misconnections from
498 both qualitative and quantitative perspective without high costs and implement timely
499 response measures.

500

501 **Acknowledgements**

502 Not applicable.

Author's contributions

All authors contributed to the study conception and design. Material preparation, data collection and analysis were performed by YH, YY, HJ and XZ. The first draft of the manuscript was written by YH and HJ. All authors commented on previous versions of the manuscript. All authors red and approved the final manuscript.

Funding

This study was financially supported by National Natural Science Foundation of China (grant no. 51979195).

Availability of data and materials

Not applicable.

Ethics approval and consent to participate

Not applicable.

Consent for publication

Not applicable.

Competing interests

The authors declare no competing financial interest.

References

1. Hoes OAC, Schilperoort RPS, Luxemburg WMJ et al (2009) Locating illicit connections in storm water sewers using fiber-optic distributed temperature sensing. Water Research 43(20):5187-5197

2. Brown E, Caraco D, Pitt R (2004) Illicit Discharge Detection and Elimination, a Guidance Manual for Program Development and Technical Assessments. 378. Center

for Watershed Protection, Maryland, U.S.

3. Irvine K, Rossi MC, Vermette S et al (2011) Illicit discharge detection and elimination: low cost options for source identification and trackdown in stormwater systems. Urban Water J. 8 (6):379-395

4. Ellis J B, Butler D (2015) Surface water sewer misconnections in England and Wales: Pollution sources and impacts. Science of the total environment 526:98-109

5. Xu ZX, Xu J, Yin HL et al (2019) Urban river pollution control in developing countries. Nature Sustainability 2:158-160

6. Xu ZX, Yin HL, Li HZ (2014) Quantification of non-stormwater flow entries into storm drains using a water balance approach. Sci. Total Environ. 487:381-388

7. Yin HL, Lu Y, Xu ZX et al (2017) Characteristics of the overflow pollution of storm drains with inappropriate sewage entry. Environmental Science and Pollution Research 24:4902-4915

8. Nakada N, Kiri K, Shinohara H et al (2008) Evaluation of pharmaceuticals and personal care products as water-soluble molecular markers of sewage. Environ. Sci. Technol. 42 (17) :6347-6353

9. Buerge IJ, Buser HR, Kahle M et al (2009) Ubiquitous occurrence of the artificial sweetener acesulfame in the aquatic environment: an ideal chemical marker of domestic wastewater in groundwater. Environ. Sci. Technol. 43 (12) :4381-4385

10. Gasser G, Rona M, Voloshenko A et al (2011) Evaluation of micropollutant tracers. II. Carbamazepine tracer for wastewater contamination from a nearby water recharge system and from non-specific sources. Desalination 273 (2) :398-404

11. Tran NH, Hu J, Li J et al (2014) Suitability of artificial sweeteners as indicators of raw

549 wastewater contamination in surface water and groundwater. Water Res. 48:443-456
550 12. Tran NH, Li J, Hu J et al (2014) Occurrence and suitability of pharmaceuticals and
551 personal care products as molecular markers for raw wastewater contamination in
552 surface water and groundwater. Environ. Sci. Pollut. Res. 21 (6) :4727-4740
553 13. Sun Q, Li M, Ma C et al (2016) Seasonal and spatial variations of PPCP occurrence,
554 removal and mass loading in three wastewater treatment plants located in different
555 urbanization areas in Xiamen, China. Environ. Pollut. 208 (Pt B) :371-381
556 14. Yang YY, Liu WR, Liu YS et al (2017) Suitability of pharmaceuticals and personal care
557 products (PPCPs) and artificial sweeteners (ASs) as wastewater indicators in the Pearl
558 River Delta, South China. Sci. Total Environ. 590:611-619
559 15. Xu ZX, Wang LL, Yin HL et al (2016) Source apportionment of non-storm water entries
560 into storm drains using marker species: Modeling approach and verification. Ecol. Indic.
561 61:546-557
562 16. Yin HL, Xie M, Zhang LY et al (2019) Identification of sewage markers to indicate
563 sources of contamination: Low cost options for misconnected non-stormwater source
564 tracking in stormwater systems. Science of the Total Environment 648:125-134
565 17. Hudson N, Baker A, Ward D et al (2008) Can fluorescence spectrometry be used as a
566 surrogate for the Biological Oxygen Demand (BOD) test in water quality
567 assessment? An example from South West England. Science of the Total Environment
568 391:149-158
569 18. Henderson RK, Baker A, Murphy KR et al (2009) Fluorescence as a potential
570 monitoring tool for recycled water systems: A review. Water Research 43:863-881
571 19. Carstea EM, Baker A, Bieroza M et al (2010) Continuous fluorescence excitation-

572 emission matrix monitoring of river organic matter. Water Research 44:5356-5366
573 20. Yu H, Song Y, Gao H et al (2015) Applying fluorescence spectroscopy and
574 multivariable analysis to characterize structural composition of dissolved organic
575 matter and its correlation with water quality in an urban river. Environ. Earth Sci.
576 73:5163-5171
577 21. Baker A, Inverarity R, Charlton M et al (2003) Detecting river pollution using
578 fluorescence spectrophotometry: Case studies from the Ouseburn, NE England.
579 Environmental Pollution 124 (1):57-70
580 22. Goldman JH, Rounds SA, Needoba JA (2012) Applications of Fluorescence
581 Spectroscopy for Predicting Percent Wastewater in an Urban Stream. Environmental
582 Science & Technology 46:4374-4381
583 23. Meng F, Huang G, Yang X et al (2013) Identifying the sources and fate of
584 anthropogenically impacted dissolved organic matter (DOM) in urbanized rivers. Water
585 Research 47:5027-5039
586 24. Li S, Zhang J, Guo E et al (2017) Dynamics and ecological risk assessment of
587 chromophoric dissolved organic matter in the Yinma River Watershed: Rivers,
588 reservoirs, and urban waters. Environmental Research 158:245-254
589 25. Zhao Y, Song K, Lv L et al (2018) Relationship changes between CDOM and DOC in
590 the Songhua River affected by highly polluted tributary, Northeast China.
591 Environmental Science and Pollution Research 25:25371–25382
592 26. Coble P.G. (1996) Characterization of marine and terrestrial DOM in seawater using
593 excitation-emission matrix spectroscopy. Marine Chemistry 51(4):325-346
594 27. Baker A , Spencer RGM(2004) Characterization of dissolved organic matter from

595 source to sea using fluorescence and absorbance spectroscopy. Science of the Total
596 Environment 333(1-3):217-232
597 28. Osburn CL, Handsel LT, Mikan MP et al (2012) Fluorescence Tracking of Dissolved
598 and Particulate Organic Matter Quality in a River-Dominated Estuary. Environ. Sci.
599 Technol.46(16):8628-8636
600 29. Zhang Y, Yin Y, Feng L et al (2011) Characterizing chromophoric dissolved organic
601 matter in Lake Tianmuhu and its catchment basin using excitation-emission matrix
602 fluorescence and parallel factor analysis. Water Research 45(16):5110-5122
603 30.Yao X, Zhang Y, Zhu G et al (2011) Resolving the variability of CDOM fluorescence in
604 Lake Taihu and its tributaries. Chemosphere 82:145-155
605 31. Song F, Wu F, Feng W et al (2019) Depth-dependent variations of dissolved organic
606 matter composition and humification in a plateau lake using fluorescence spectroscopy.
607 Chemosphere 225:507-516
608 32. Lü WW, Yao X, Shao KQ et al (2019) Unraveling the sources and fluorescence
609 compositions of dissolved and particulate organic matter (DOM and POM) in Lake
610 Taihu, China. Environmental Science and Pollution Research 26:4027-4040
611 33. Henderson RK, Baker A, Murphy KR et al (2009) Fluorescence as a potential
612 monitoring tool for recycled water systems: A review. Water Research 43:863-881
613 34. Baker A, Lamont-black J (2001) Fluorescence of Dissolved Organic Matter as a Natural
614 Tracer of Ground Water. Groundwater 39(5):745-750
615 35. Chen H, Liao Z, Gu X et al (2017) Anthropogenic Influences of Paved Runoff and
616 Sanitary Sewage on the Dissolved Organic Matter Quality of Wet Weather Overflows:
617 An Excitation−Emission Matrix Parallel Factor Analysis Assessment. Environ. Sci.

618 Technol 51:1157-1167
619 36. Holbrook RD, Derose PC, Leigh SD et al (2006) Excitation–emission matrix
620 fluorescence spectroscopy for natural organic matter characterization: a quantitative
621 evaluation of calibration and spectral correction procedures. Applied Spectroscopy 60
622 (7), 791–799
623 37. Ye Z (2012) Study on the correction of dry-weather pollutants inappropriate entry into
624 storm drainage based on pipe hydrodynamic model. Master Thesis, Tongji University,
625 Shanghai **(in Chinese)**
626 38. Hudson N, Baker A, Reynolds D et al (2007) Fluorescence Analysis of Dissolved
627 Organic Matter in Natural, Waste and Polluted Waters – A Review. River Research and
628 Applications 23:631-649
629 39. S Sharifi, M M Haghshenas, T Deksissa et al (2014) Storm Water Pollution Source
630 Identification in Washington, DC, Using Bayesian Chemical Mass Balance Modeling,
631 Journal of Environmental Engineering 140, 04013015
632 40. J A Vrugt (2016) Markov chain Monte Carlo simulation using the DREAM software
633 package: Theory, concepts, and MATLAB implementation, Environmental Modelling
634 & Software 75, 273-316
635 41. Chen MF, Wu J, Lv YL et al (2008) Fluorescence Properties of Municipal Wastewater.
636 Acta Optica Sinica 28(3):578-582 **(in Chinese)**
637 42. Parlanti E, Worz K, Geoffroy L et al (2000) Dissolved organic matter fluorescence
638 spectroscopy as a tool to estimate biological activity in a coastal zone submitted to
639 anthropogenic inputs. Organic Geochemistry 31(12): 1765–1781
640 43. Ji GH (2015) Investigation of hydrophytes of slow flow water bodies to guide

641 ecological restoration in Shanghai. Ph.D Dissertation, Tongji University, Shanghai **(in**
642 **Chinese)**
643 44. Ren BW, Zhao WH, Wang JT et al (2007) Three-Dimensional Fluorescence
644 Characteristic of Dissolved Organic Matter in Marine Mesocosm Experiment in
645 Jiaozhou Bay, China. Environmental Science 28(4):712-718 **(in Chinese)**
646 45. DM Reynolds (2002) The Differentiation of Biodegradable and Non-biodegradable
647 Dissolved Organic Matter in Wastewaters Using Fluorescence Spectroscopy. Journal
648 of Chemical Technology & Biotechnology 77(8):965-972
649
650
651

Figures

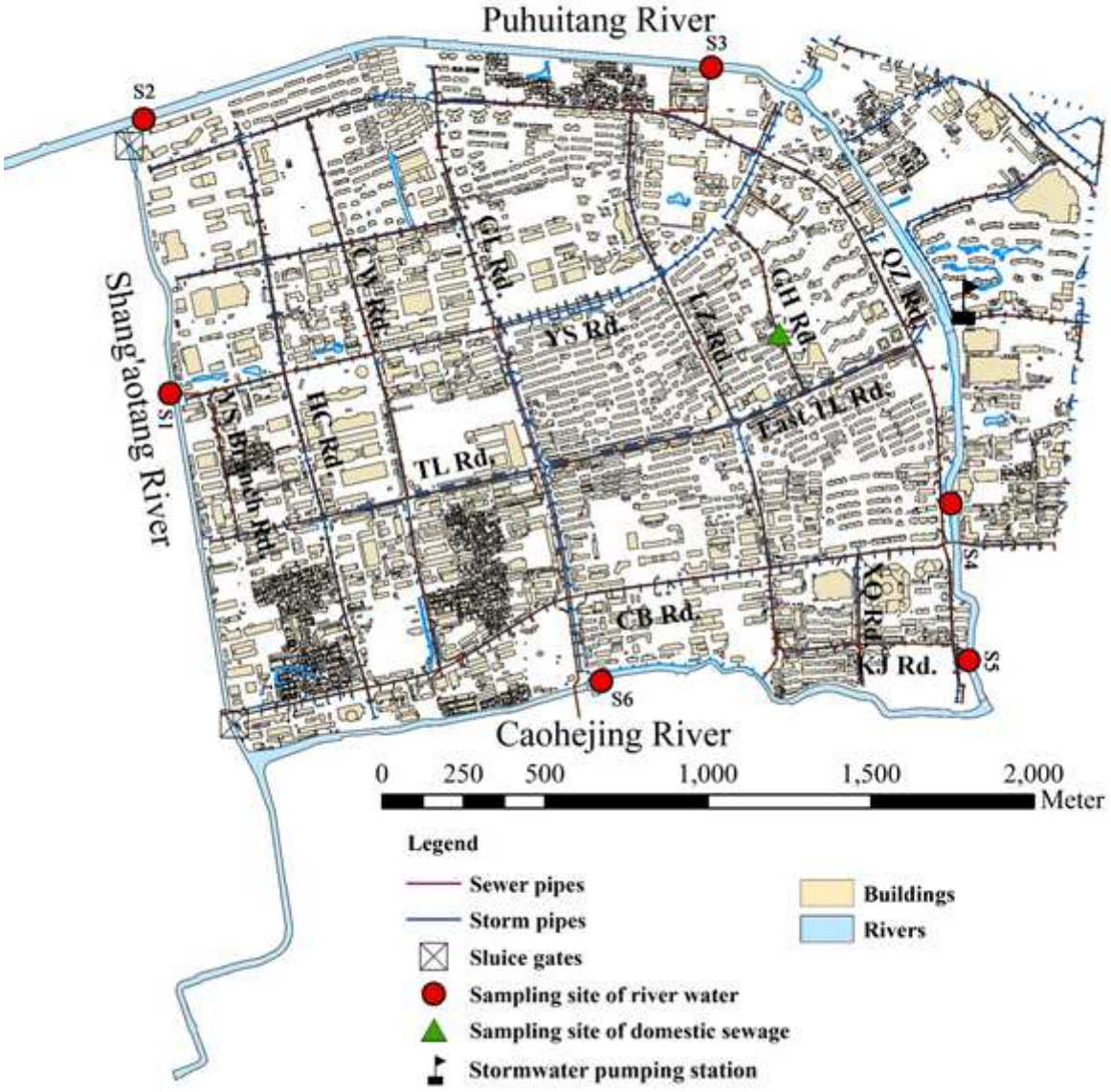

Figure 1

Study site description

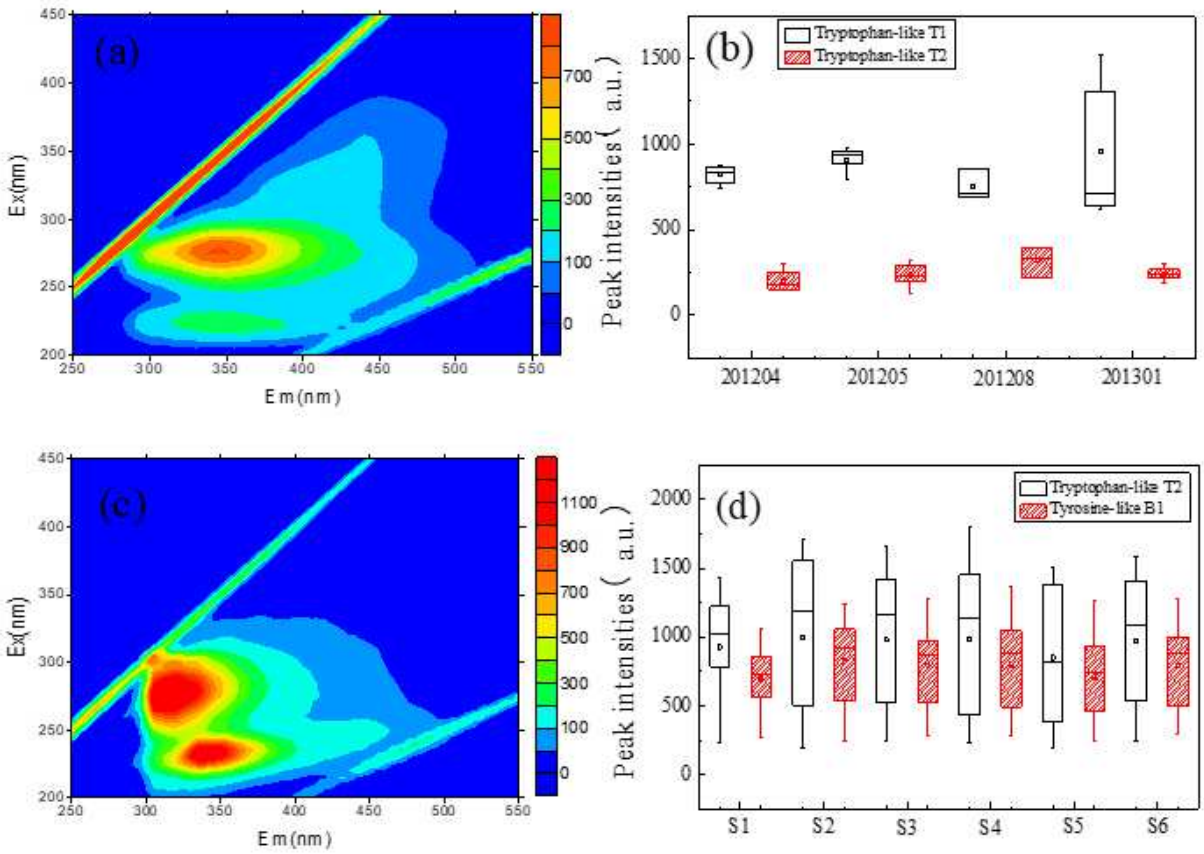

Figure 2

Detected EEMs for the domestic sewage and urban river water samples: (a) typical EEM of untreated domestic sewage; (b) fluorescent peak intensities of domestic sewage samples; (c) typical EEM of urban river water; (d) fluorescent peak intensities of urban river water at six sampling stations.

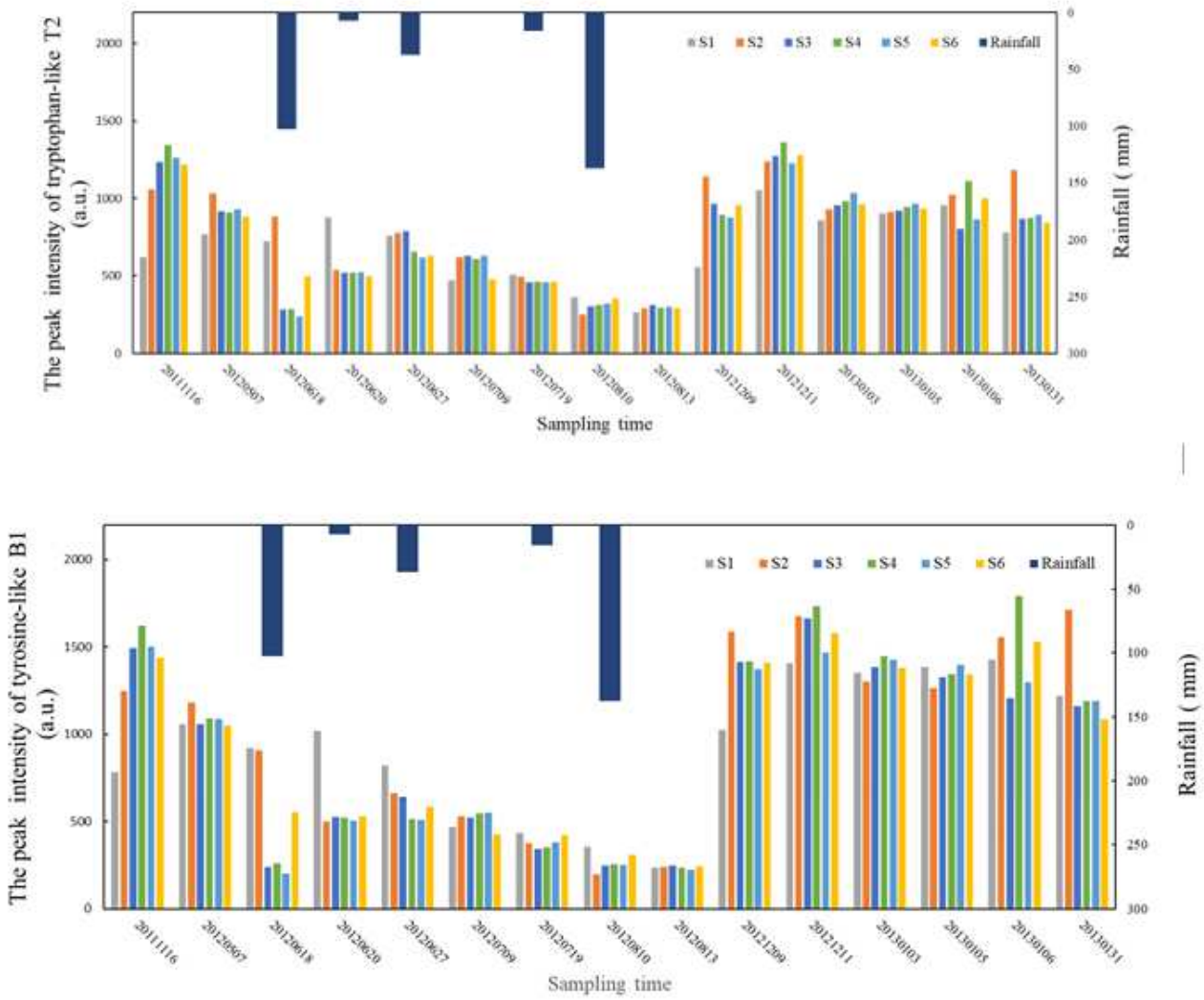

Figure 3

Detected fluorescence intensities at six sampling sites of the urban river water.

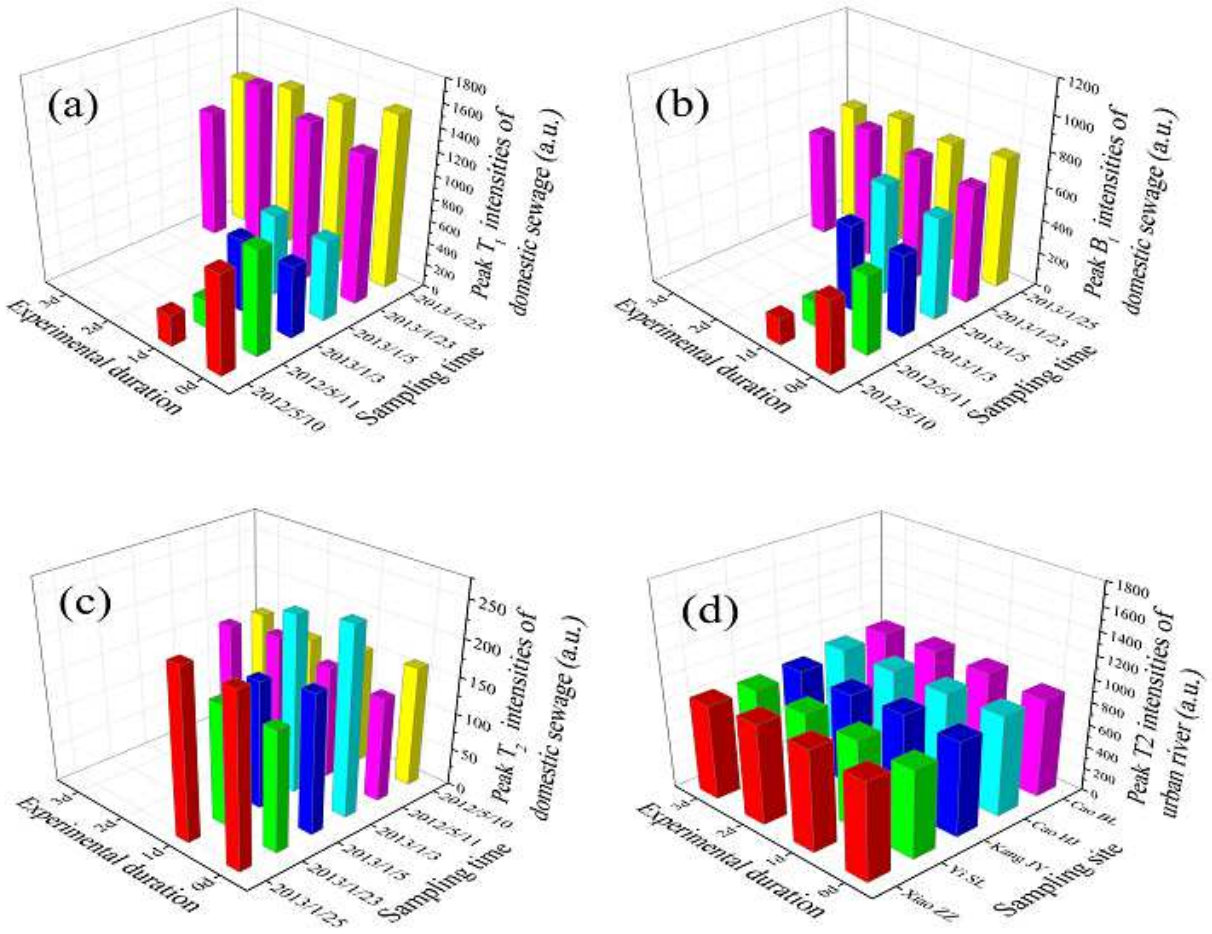

Figure 4

Changes of fluorescence peak intensities of domestic sewage and urban river water samples within the experimental duration.

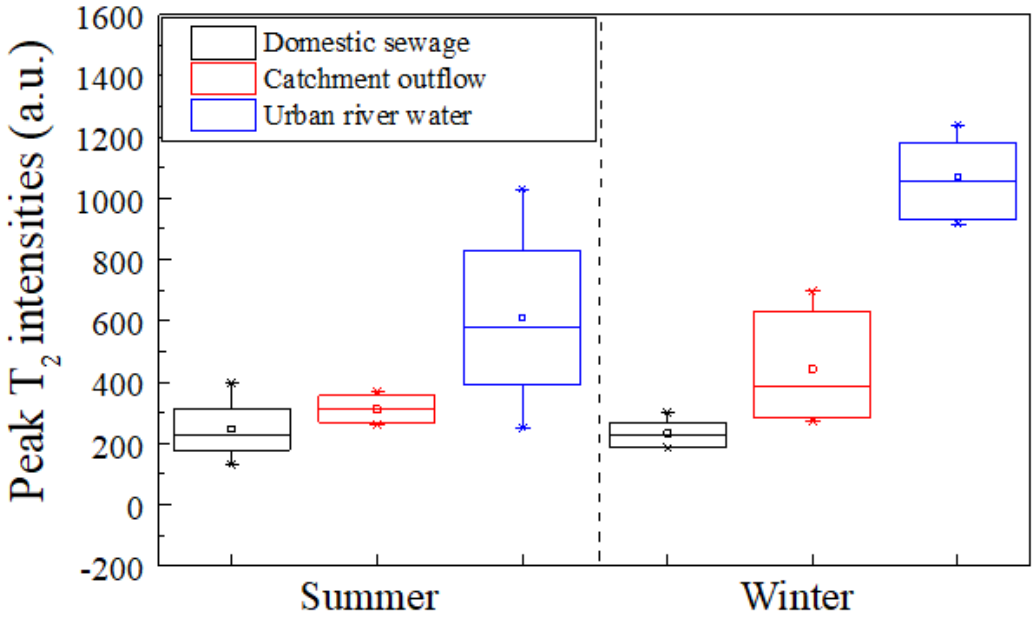

Figure 5

Comparison of fluorescence peak T2 intensities for the samples among river water, domestic sewage and catchment outflow.

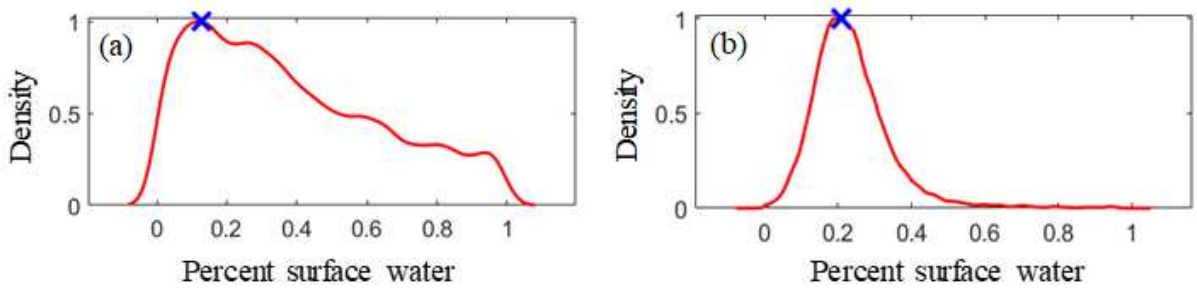

Figure 6

Maximum a posteriori probability (MAP) estimate for the percentage share of river water backflow into the storm drains on dry-weather days: (a) summer season; (b) winter season.

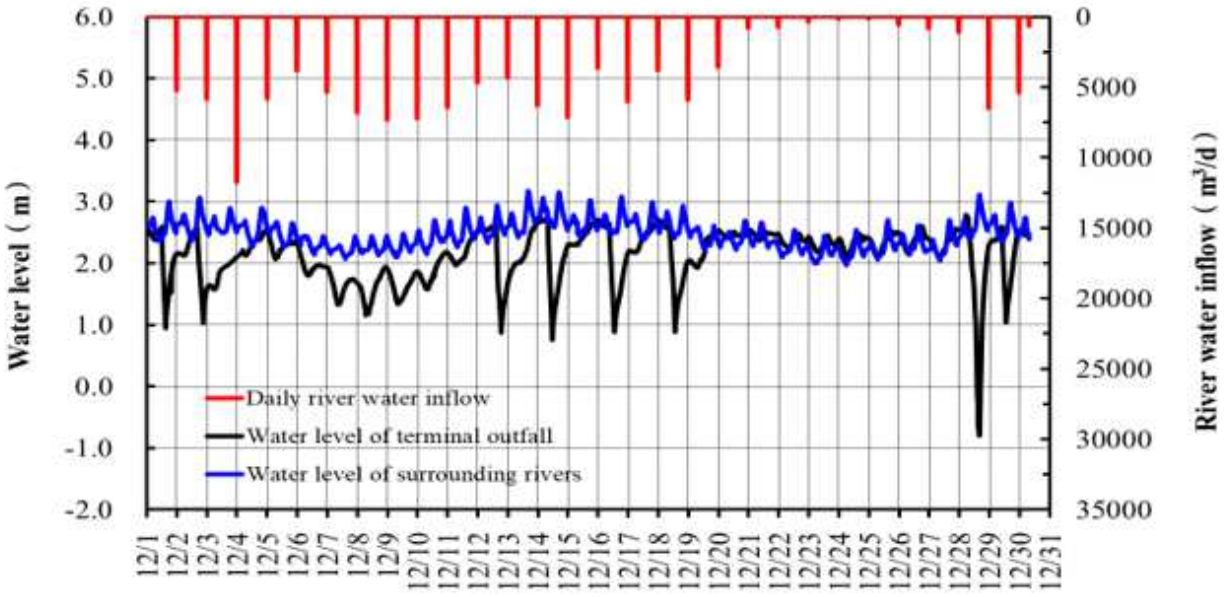

Figure 7

Estimated daily river water inflow into storm drains based on real-time water level between river and catchment outfall in winter season period.

Supplementary Files

This is a list of supplementary files associated with this preprint. Click to download.

- Supportinginformation.docx